PERFORMANCE OF MULTIPLE COMBINED PROFILE COLD-FORMED STEEL COLUMN

ZAMZAMI SEPTIROPA

A thesis submitted in fulfilment of the
requirements for the award of the degree of
Doctor of Philosophy

School of Civil Engineering
Faculty of Engineering
Universiti Teknologi Malaysia

APRIL 2021

DEDICATION

This thesis is dedicated to my parents, who taught me that the best kind of knowledge to have is that which is learned for its own sake. It is also dedicated to my mother, who taught me that even the largest task can be accomplished if it is done one step at a time.

ACKNOWLEDGEMENT

In preparing this thesis, I was in contact with many people, researchers, academicians, and practitioners. They have contributed towards my understanding and thoughts. In particular, I wish to express my sincere appreciation to my first main thesis supervisor, Professor Dr. Mohd Hanim bin Osman, for encouragement, guidance, critics and friendship. I am also very thankful to my second main thesis supervisor Assoc. Prof. Dr Arizu bin Sulaiman and my co-supervisor Professor Dr Ahmad Baharuddin bin Abd. Rahman for their guidance, advices and motivation. Without their continued support and interest, this thesis would not have been the same as presented here.

I am also indebted to Universitas Muhammadiyah Malang (UMM) for funding my Ph.D. study. Technicians at Material and Structure Laboratory of Civil Engineering UTM, Librarians at UTM also deserve special thanks for their assistances throughout the research.

My fellow postgraduate student should also be recognised for their support. My sincere appreciation also extends to all my colleagues and others who have provided assistance at various occasions. Their views and tips are useful indeed. Unfortunately, it is not possible to list all of them in this limited space. I am grateful to all my family member.

ABSTRACT

In the construction of low-rise buildings, cold-formed steel (CFS) as column is rarely used even though it is an important component. Previous studies have shown that the main weakness of CFS is its buckling behaviour due to the thin nature of CFS section. By combining multiple similar profiles to form a new profile using self-drilling screw connectors, strong column can be obtained in terms of the cross-sectional capacity and buckling resistance. This research investigates the performance of multiple combined profile columns, to obtain the relevant limits for the capacity design factor of multiple combined profile sections. To achieve this research aim, theoretical analysis and experimental works were carried out based on C7575 C-Channel profile. Firstly, the testing of the material properties of the C7575 was conducted, to be followed by the analysis and testing of single profile member capacity with variations in length of 300, 500, 1000, 1750 and 2500 mm. Then, analysis of the combined profiles that comprises of double-back-to-back (dBB), double-lips-to-lips (dLL) and double-flange-to-flange (dFF) profiles were performed to obtain the new cross-sectional capacity. To obtain the ideal spacing of self-drilling screw connector, a compressive test was performed on the combined dFF and combined dBB profiles with variations in spacing of 25, 50, 75, 100 and 125 mm using 300 mm length sample. The combined dFF and dBB profiles were assembled and arranged to form several multiple combination profiles, namely 2dFF, 4dFF, 6dFF, and 8dFF to obtain the adequate strength and performance for low-rise building column applications. It is found that C7575 profile possess the ultimate strength, f_u = 616.27 N/mm^2 , yield strength, f_y = 597.93 N/mm^2 , modulus of elasticity, E = 209 GPa and shear modulus, G = 80.38 GPa. It also found that, double-back-to-back (dBB) and double-flange to-flange (dFF) are the ideal configurations for multiple combined profiles of CFS. The patterns yielded an increase in the cross-sectional capacity with a ratio ranging from 1.7 to 1.8. As for the spacing of screws, the ideal distance for dBB is 75 mm to 125 mm while for dFF, it is 75 mm to 100 mm. Observations on the performance of the eight-double-flange-to-flange (8dFF) multiple combined profile shows that the profile did not experience any rotation deformation. In general, the recommended value of imperfection factor, α for the C-channel profile type is 0.34 while for other types of profile CFS, the value of α can be taken as 0.76. The α value of 0.76 even though it produces a match between the results of theoretical and experimental calculations, it is too confident for a calculation. Based on the theoretical formulation, it is found that a new value of α for 8dFF multiple combined profile is equal to 1.14. This new value of α is therefore proposed, to determine the appropriate reduction factors for buckling about y axis, χ_y and z axis, χ_z for the type of 8dFF multiple combined profile. The research concluded that 8dFF multiple combined profile can be used efficiently as column for low-rise building structure.

ABSTRAK

Dalam pembinaan bangunan bertingkat rendah, keluli terbentuk sejuk (CFS) sebagai tiang jarang digunakan walaupun ianya merupakan komponen yang penting. Kajian terdahulu menunjukkan bahawa kelemahan utama CFS adalah kelakuan lengkukannya yang disebabkan oleh sifat bahagian CFS yang tipis,. Dengan penggabungan dan pemasangan beberapa profil individu yang serupa bagi membentuk satu profil baharu menggunakan penyambung skru gerudi-diri, tiang yang memadai dapat diperolehi dari segi kapasiti keratan rentas dan rintangan lengkukan. Penyelidikan ini bertujuan untuk mengkaji prestasi struktur tiang profil gabungan berganda, bagi mendapatkan had yang relevan yang dapat digunakan sebagai faktor reka bentuk kapasiti keratan-keratan profil gabungan berganda. Untuk mencapai tujuan penyelidikan ini, analisis secara teori dan kerja ujikaji dilakukan dengan berdasarkan kepada profil C7575 C-Channel. Pertama, penyiasatan sifat bahan C7575 dilakukan, diikuti dengan analisis dan pengujian kapasiti anggota profil tunggal dengan variasi panjang 300, 500, 1000, 1750 dan 2500 mm. Kemudian, analisis profil gabungan C7575 yang terdiri daripada profil *double-back-to-back* (dBB), *double-lips-to-lips* (dLL) dan *double-flange-to-flange* (dFF) dilakukan untuk mendapatkan kapasiti keratan rentas yang baharu. Dalam pada itu, untuk mendapatkan jarak ideal penyambung skru gerudi-diri, ujian mampatan dilakukan pada profil gabungan dFF dan gabungan dBB dengan variasi jarak 25, 50, 75, 100 dan 125 mm. Tiga sampel dengan panjang 300 mm untuk setiap variasi jarak telah diuji. Selepas itu, gabungan profil dFF dan dBB dipasang dan disusun untuk membentuk beberapa profil gabungan berganda iaitu 2dFF, 4dFF, 6dFF, dan 8dFF bagi mendapatkan kekuatan dan prestasi yang mencukupi untuk aplikasi tiang bangunan bertingkat rendah. Profil C7575 didapati memiliki kekuatan muktamad, f_u = 616.27 N/mm^2 , kekuatan alah, f_y = 597.93 N/mm^2 , modulus keanjalan, E = 209 GPa dan modulus ricih, G = 80.38 GPa. Corak yang dipilih untuk menggabungkan profil seperti *double-back-to-back* (dBB) dan *double-flange-to-flange* (dFF) adalah konfigurasi yang sesuai untuk profil gabungan berganda CFS. Corak-corak ini menghasilkan peningkatan kapasiti keratan rentas dengan nisbah antara 1.7 hingga 1.8. Bagi jarak antara skru pula, jarak yang ideal untuk dBB ialah 75 mm hingga 125 mm sementara untuk dFF adalah 75 mm hingga 100 mm. Pemerhatian terhadap prestasi profil gabungan berganda *eight-double-flange-to-flange* (8dFF) menunjukkan bahawa profil tersebut tidak mengalami ubah bentuk putaran. Secara umum, nilai faktor ketidaksempurnaan, α yang disarankan untuk jenis profil C-Channel adalah 0.34 sementara untuk jenis-jenis lain, nilai α boleh diambil sebagai 0.76. Nilai α bersamaan dengan 0.76 kelihatan masih dapat menghasilkan kesepakatan yang baik antara hasil pengiraan teori dan ujikaji. Walau bagaimanapun, melalui proses pengiraan ke belakang, rumusan telah menghasilkan nilai α yang baharu untuk profil gabungan berganda 8dFF bersamaan dengan 1.14. Oleh yang demikian, nilai α yang baharu ini dicadangkan, dan dapat digunakan untuk menentukan factor-faktor pengurangan yang sesuai bagi lengkukan paksi y, χ_y dan paksi z, χ_z untuk jenis profil gabungan berganda 8dFF. Penyelidikan ini menyimpulkan bahawa profil gabungan berganda 8dFF boleh digunakan dengan berkesan sebagai tiang untuk struktur bangunan bertingkat rendah.

TABLE OF CONTENTS

TITLE	PAGE
DECLARATION	**iii**
DEDICATION	**iv**
ACKNOWLEDGEMENT	**v**
ABSTRACT	**vi**
ABSTRAK	**vii**
LIST OF TABLES	**xii**
LIST OF FIGURES	**xv**
LIST OF ABBREVIATIONS	**xxiii**
LIST OF SYMBOLS	**xxiv**
LIST OF APPENDICES	**xxvii**
CHAPTER 1 INTRODUCTION	**1**
1.1 Overview	1
1.2 Background of the Study	4
1.3 Problem Statement	6
1.4 Objectives	7
1.5 Scope of the Study	8
1.6 Significances and Original Contributions of This Study	9
1.7 Organization of Thesis	9
CHAPTER 2 LITERATURE REVIEW	**11**
2.1 Mechanical Properties of CFS	11
2.1.1 Yield Stress, Tensile Stress, and Stress-Strain Curves of CFS	11
2.1.2 Modulus of Elasticity and Yield strength	13
2.1.3 Ductility	13
2.2 Structure Compression Members and Criteria	15
2.2.1 Stiffness of the Press Element	15
2.2.1.1 Yielding	15

2.2.1.2 Elastic Local Buckling Stress of Plate 16
2.2.1.3 Postbuckling Strength and Effective Design Width 17
2.3 CFSBuckling Types 24
2.4 CFS Section as Single Unit Combined Profile Column 25
2.5 Analytical and Experimental Studies on CFS 27
2.6 Plate Stiffeners on CFS Compression Members 29
2.7 Capacity of Strengthened Steel Sections 30
2.8 Combined Profile CFS 34
2.9 Gap of Research 38

CHAPTER 3 RESEARCH METHODOLOGY 39
3.1 Overview 39
3.2 Materials of CFS 40
3.3 Model Test 41
3.3.1 Combined Profile as Compression Member 42
3.3.2 Self-drilling Screws as Connections for Combined Profile CFS 46
3.3.3 Combined Profile CFS as a Column 53
3.4 Chapter Remarks 57

CHAPTER 4 PERFORMANCE OF COMBINED PROFILE COLD-FORMED COMPRESSION MEMBERS 59
4.1 Mechanical Properties 59
4.1.1 Experimental Test of Tensile Strength and Yield Strength 59
4.1.2 Experimental Test of Modulus of Elasticity 66
4.1.3 Experimental Results of Tensile Strength, Yield Strength, and Modulus of Elasticity 73
4.1.3.1 Experimental Remarks 75
4.2 Design Calculation of the Cross-Sectional Capacity of the C7575 Profile 75
4.3 Section Properties Analysis 80
4.4 Experimental Program 98

4.4.1 Specimen, Test Procedure and Results 98
4.4.1.1 Single Profile C7575 103
4.4.1.2 Double Profile Back-to-Back and Lip-to-Lip 104
4.4.1.3 Double Profile Flange-to-Flange, dFF 109
4.5 Combined Profile 111
4.5.1 Combined Profile with Screws as Connectors 112
4.5.2 Experimental Tests for Screw Distance in Combined Profiles 113
4.5.2.1 Test Set-Up and Procedures 113
4.5.2.2 Experimental Results 121
4.6 Discussion 122
4.7 Chapter Remarks 124

CHAPTER 5 STRENGTH OF COMBINED PROFILE AS COLUMN 127

5.1 Combined Profile as a Column 127
5.1.1 Single Profile C7575 as Compression Member 128
5.1.1.1 Single Profile L1750 128
5.1.1.2 Single Profile L2500 131
5.1.2 Double Profile Flange-to-Flange (dFF) (Closed Profile) 134
5.2 Combined profile (dFF) as columns for low-rise building 142
5.2.3 Eight Double Profile Flange-to-Flange (8dFF) 151
5.2.3.1 Combine 8dFF L1000 mm 156
5.2.3.2 Combined 8dFF L1750 mm 158
5.2.3.3 Combined profile 8dFF L2500 mm 163
5.3 Combined Profile Applied for Columns 169
5.3.1 Strength Capacity of Combined Profile, 8dFF 169
5.3.1.1 Resistance Check of the Cross-section Combined Profile 8DFF 173
5.3.1.2 Imperfection Factor *(α)* for Combined Profile 8dFF 179
5.3.2 Applied Program 181
5.4 Chapter Remarks 190

CHAPTER 6 CONCLUSION **193**

6.1 Introduction 193

6.2 Conclusions 194

6.3 Future Works 195

REFERENCES **197**

APPENDIXS **203**

LIST OF PUBLICATIONS **251**

LIST OF TABLES

TABLE NO.	TITLE	PAGE
Table 2.1	Local buckling coefficient (Yu, 2010)	17
Table 2.2	Technical data of screws, ultimate strength pullout tension, lb (kN) (www.hilti.com.ca)	34
Table 2.3	Column buckling curves and imperfection factors α (based on Tables 6.1 and 6.2 of BS EN 1993 -1-1) (Gardner, 2011)	36
Table 3.1	Section dimensions and properties	40
Table 3.2	Types of profiles combined and variation screws distance	47
Table 3.3	Technical data of screws, ultimate strength pullout tension, lb (kN) (www.hilti.com.ca)	48
Table 4.1	Dimensions of tensile test coupons	61
Table 4.2	Test results for coupon C-section C7575, t = 0.75 mm	63
Table 4.3	Yield strength, f_y, based on ratio calculations	64
Table 4.4	Dimensions of tensile test coupons C7575	68
Table 4.5	Results of tensile test C7575, ultimate strength, f_u, and yield strength, f_y	70
Table 4.6	Tensile strength (P/A) and modulus of elasticity (E)	71
Table 4.7	Modulus of elasticity calculation	71
Table 4.8	Calculation of ultimate strength, fu	72
Table 4.9	Calculation of yield strength, fy	72
Table 4.10	Calculation Results Profile C7575	78
Table 4.11	Material properties of CFS C7575	79
Table 4.12	Calculation results for all profiles' dimensions	83
Table 4.13	Material Properties of CFS	87
Table 4.14	Single Profile C7575	88
Table 4.15	Double profile back-to-back C7575, dBB	89
Table 4.16	Double profile flange-to-flange C7575, dFF	90

Table 4.17	Double profile lip-to-lip C7575	91
Table 4.18	Comparison profile for single, dBB, dFF and dLL	92
Table 4.19	Double profile 2 close (2dFF)	94
Table 4.20	Combined 4 close profile (4dFF)	95
Table 4.21	Combine 8 close profile (8dFF)	96
Table 4.22	Ratio of strength differences between SC and combined profiles	97
Table 4.23	Comparison between the calculations and experiments C7575	104
Table 4.24	Comparison between calculations and experiments for dBB and dLL	108
Table 4.25	Comparison between the calculation and experiment for the double profile flange-to-flange, dFF	110
Table 4.26	Technical data of screws and ultimate strength pullout tension, lb (kN) (www.hilti.com.ca)	113
Table 4.27	Type of combined profile with variation screws distance	114
Table 5.1	Results of compression test profile C7575	133
Table 5.2	Comparison of results for single C7575 vs double flange-to-flange (dFF)	140
Table 5.3	Calculation for double profile based on EC3	141
Table 5.4	Experiments vs calculation for double profile (dFF)	141
Table 5.5	Calculation results of 2dFF	148
Table 5.6	Calculation results of 4dFF	150
Table 5.7	Calculation results of 8dFF	152
Table 5.8	Capacity of different multiple profiles formed by C7575 (l_e=2500 mm)	154
Table 5.9	Capacity of difference multiple profiles formed by C7575	155
Table 5.10	Calculation results for 8dFF	171
Table 5.11	Comparison of Calculation vs Experiment for combined 8dFF (fy = 550 N/mm2& E = 205 GPa)	172
Table 5.12	Imperfection factor for buckling curve	177

Table 5.13	Recommended value for the lateral-torsional buckling curve for the cross-section	179
Table 5.14	Calculation reduction factor, ξ, and □ value for 8dFF	183
Table 5.15	Calculation □ value for 8dFF	185
Table 5.16	Calculation of reduction factor,	187
Table 5.17	Comparison of results when Nb,RD α=0.76 and Nb,RD α=1.14	189

LIST OF FIGURES

FIGURE NO.	TITLE	PAGE
Figure 1.1	(a). Wall-system installation (Alliance, 2007), (b). Single story building (Newfabksa, 2007)	2
Figure 1.2	(a) A CFS wall system (Alliance, 2007) and (b) a multi-story building structure used CFS as the wall system's main structure from steel profiles (www.greenmaltese.com).	3
Figure 1.3	(a) Stub column test: details on the specimen, (b) the specimen before testing, and (c) typical failure due to local and distortional buckling (Bernuzzi and Maxenti, 2015).	5
Figure 1.4	(a) Single and triple profile behaviour (torsional buckling dominated) and (b) double profile behaviour (local buckling dominated)	5
Figure 2.1	Stress-strain curve of strip or steel sheet: (a) sharp yielding and (b) gradual yielding (Yu, 2010)	12
Figure 2.2	Local buckling of compression elements (Wei-Wen Yu, 2011).	15
Figure 2.3	A simply supported square plate under compression (Dubina, 2012).	16
Figure 2.4	Stress distribution of a plate element (Yu, 2011).	18
Figure 2.5	Stress distribution in a compression element according to Yu (1999).	18
Figure 2.6	Stress distribution in a simply supported plate (Dubina, 2012).	19
Figure 2.7	Changes in effective width with respect to maximum stress	19
Figure 2.8	Relationship between reduction factor, ρ, and relative plate slenderness, λ_p	23
Figure 2.9	Overall short column instability and local buckling (Chen and Deng, 2014)	25
Figure 2.10	Built-up CFS section battened columns in the experiment done by Dabaon *et al.* (2015)	26

Figure 2.11	Eccentric axial load and failure mode of a CFS battened column (El Aghoury *et al.*, 2015)	27
Figure 2.12	Methods in analysing CFS: a) EWM and b) DSM (Schafer, 2008)	28
Figure 2.13	(a) Von-Mises stress contour at ultimate load and (b) a comparison of failure model test and finite element modelling (Anbarasu, 2016)	29
Figure 2.14	(a) Set-up for testing CFS with plate stiffness and (b) details of two full web side plates (Keerthan and Mahendran, 2015)	30
Figure 2.15	End distance, edge distance, and spacing for fasteners and spot welds (BS.EN1993-1-3, 2006)	31
Figure 2.16	Schematic diagram of truss connections with (a) a 45° truss connection specimen and (b) a 90° truss connection (Zeynalian *et al.*, 2016).	32
Figure 2.17	Variations of screw configurations (Bondok and Salim, 2017)	32
Figure 2.18	Type of screw: Philips Pan Head, PPH and hex washer head, HWH (www.hilti.com.ca)	33
Figure 2.19	Comparison of failure of three stitches specimens (Vijayanand and Anbarasu, 2017)	34
Figure 2.20	Comparison of experimental and FEA and Column test of built-up closed section (Young, 2008)	35
Figure 2.21	Column buckling curves in BS EN 1993 -1-1	36
Figure 2.22	Comparison of failure modes between experimental and finite element analysis and corresponding built-up sections (Zhang and Young, 2015)	37
Figure 3.1	Research stages for studying combined profile CFS-based columns	39
Figure 3.2	(a) C-channel C7575 and (b) specimen dimensions for metal sheets based on the requirements of ASTM E8	41
Figure 3.3	Building framing system	42
Figure 3.4	Position of combined profile CFS as column	42
Figure 3.5	Flowchart representing the basic design of compression member	43
Figure 3.6	The model test of CFS as a compression member: (a) a single C7575, (b) a combined profile flange-to-flange	

	(dFF), (c) a combined profile back-to-back (dBB), and (d) a combined profile lip-to-lip (dLL)	44
Figure 3.7	Set-up of the compression test by Craveiro (2016b)	45
Figure 3.8	Set-up of the test of the short column by El Aghoury (2017)	45
Figure 3.9	Set-up test for compression test C-Channel profile and combined profile CFS	46
Figure 3.10	Types of self-drilling screws (HILTI, 2015)	47
Figure 3.11	dFF specimens with various screw distances	49
Figure 3.12	dBB specimens with various screw distances	50
Figure 3.13	Test specimens by Liao (2017)	51
Figure 3.14	Experimental set-up by Liao (2017)	51
Figure 3.15	Compression testing machine (Tinius-Olsen)	52
Figure 3.16	Flowchart of a combined profile as a compression member	52
Figure 3.17	Flowchart analyses and experiment combined profile as a column	53
Figure 3.18	Sample of a combined profile as a column	54
Figure 3.19	Set-up for the experimental work on a combined profile (Craveiro et al., 2016a)	55
Figure 3.20	Bottom base with a hydraulic jack and end support (Craveiro et al., 2016a)	55
Figure 3.21	Set-up testing column	56
Figure 3.22	Position and end-support of the sample	57
Figure 4.1	Specimen model for the tensile test: sheet type = ½ inch (12.5 mm) wide	59
Figure 4.2	(a) Original material CFS, (b) section CFS C7575, (c) web section, and (d) flange section	60
Figure 4.3	(a) Coupon of original material, (b) coupon of the web section, and (c) coupon of the flange section	60
Figure 4.4	Tensile test with a universal testing machine (Instron-5567) (50 kN)	61
Figure 4.5	Coupons tensile test after testing	62
Figure 4.6	Tensile test results of the original material (TO)	65

Figure 4.7	Stress-strain curve of the web section, C-channel C7575 (TW)	65
Figure 4.8	Stress-strain curve of the flange section, C-channel C7575 (TF)	66
Figure 4.9	Tensile test Shimadzu with an extensometer	67
Figure 4.10	Tensile test machine Shimadzu (250 kN)	67
Figure 4.11	Coupon tensile test of C Channel C75	68
Figure 4.12	Stress-strain curve for C7575 for all specimens	69
Figure 4.13	Detailed stress-strain curves for C7575 on selected specimens	70
Figure 4.14	Profile C-channel C7575, t = 0.75 mm	76
Figure 4.15	Graphic calculation results profile C7575	79
Figure 4.16	Dimension of C-channel C7575 and C10010	80
Figure 4.17	Dimension of C-channel C15012 and C20015	80
Figure 4.18	C-channel C25019 and C30024 Dimensions	81
Figure 4.19	Effective Area, A_{eff}, of C7575, and C10010	81
Figure 4.20	Effective Area, A_{eff}, of C7575, C10010, and C15012	82
Figure 4.21	Effective Area, A_{eff}, of C25019 and C30024	82
Figure 4.22	Relationship between A_{eff}/A_g ratio and thickness profile, t 83	
Figure 4.23	Relationship between A_{eff} (mm^2) and profile thickness, t (mm)	84
Figure 4.24	Relationship between effective height, h_{eff} (mm), and profile thickness, t (mm)	85
Figure 4.25	Relationship between effective width, b_{eff} (mm), and profile thickness, t (mm)	85
Figure 4.26	Relationship between effective lips, c_{eff} (mm), and profile thickness, t (mm)	86
Figure 4.27	Combined C7575 profiles	87
Figure 4.28	Single Profile C7575	88
Figure 4.29	Double profile back-to-back C7575	89
Figure 4.30	Double profile flange-to-flange C7575	90
Figure 4.31	Double profile lip-to-lip C7575	91

Figure 4.32	Double profile comparison	92
Figure 4.33	Double profile back-to-back (dBB) and flange-to-flange (dFF), joined with screws	93
Figure 4.34	Double profile combination dFF2, 4dFF and 8dFF	94
Figure 4.35	Combined 2 close profile (2dFF)	95
Figure 4.36	Combined 4 close profile (4dFF)	96
Figure 4.37	Combine 8 close profile (8dFF)	97
Figure 4.38	Combination of Combined C7575	98
Figure 4.39	dBB and dFF samples (l_e = 300 mm)	99
Figure 4.40	Double profile back-to-back and double profile flange-to-flange or closed profile	99
Figure 4.41	Compression test machine (Tinius-Olsen)	100
Figure 4.42	Support model by Craveiro (2016)	101
Figure 4.43	Test model by Craveiro (2016) for combined profile	101
Figure 4.44	Model test for compression by Kalavagunta (2013)	102
Figure 4.45	Model test for compression by Zeng (2015)	102
Figure 4.46	Compressive test procedure for single profile C7575	103
Figure 4.47	Compression results of single profile C7575	103
Figure 4.48	Double profile back-to-back, C7575	105
Figure 4.49	Local buckling near the load position	106
Figure 4.50	Double profile back-to-back specimen with screw connections at mid-height	106
Figure 4.51	Double profile lip-to-lip specimen with batten in the middle	107
Figure 4.52	Experiment results of combined double profile dBB and dLL	107
Figure 4.53	Double profile flange-to-flange, C7575	109
Figure 4.54	Experimental results of double profile flange-to-flange, dFF	110
Figure 4.55	Type of screw: Philips pan head (PPH) and hex washer head (HWH) (www.hilti.com.ca)	112
Figure 4.56	Test set-up of the combined profile dFF and dBB on the compression test machine	114

Figure 4.57	Calculation results of the double profile back-to-back and double profile flange-to-flange models	116
Figure 4.58	Graphic and picture testing results for dFF300-S25	117
Figure 4.59	Graphic and picture testing results for dFF300-S50	117
Figure 4.60	Graphic and picture testing results for dFF300-S75	117
Figure 4.61	Graphic and picture testing results for dFF300-S100	118
Figure 4.62	Graphic and picture testing results for dFF300-S125	118
Figure 4.63	Screw distance and maximum load for the double profile flange-to-flange (dFF)	119
Figure 4.64	Graphic and picture testing results for dBB300-S25	119
Figure 4.65	Graphic and picture testing results for dBB300-S50	120
Figure 4.66	Graphic and picture testing results for dBB300-S75	120
Figure 4.67	Graphic and picture testing results for dBB300-S100	120
Figure 4.68	Graphic and picture testing results for dBB300-S125	121
Figure 4.69	Screw distance and maximum load for dBB300	121
Figure 5.1	Variation combined profile section C7575	127
Figure 5.2	Single profile C7575 in different lengths for testing	128
Figure 5.3	Single profile C7575 with length, l_e = 1750 mm	129
Figure 5.4	Compressive test of single C7575 for l_e = 1750 with pinned end supports.	129
Figure 5.5	Compression results single C7575 for l_e = 1750 mm: (a) vertical deformation and (b) horizontal deformation.	130
Figure 5.6	Loading test process of single profile C7575: (a) L2500-01 and (b) L2500-02	131
Figure 5.7	Compression test results for single C7575 with l_e = 2500 mm: (a) vertical deformation L2500-01 and (b) vertical deformation L2500-02.	132
Figure 5.8	Failure mode of the single profile with l_e = 2500 mm	133
Figure 5.9	Compression test single profile C7575 in various length.	134
Figure 5.10	Specimens used in the experiment	135
Figure 5.11	Double profile flange-to-flange (dFF) L1000mm	136
Figure 5.12	Strength capacity of double profile dFF L1000	136

Figure 5.13	(a) and (b) Testing process dFF L1750mm, (c) deformation of dFF L1750, and (d). tetsing results for dFF 1750	137
Figure 5.14	Load vs deformation for dFF L1750	138
Figure 5.15	Testing process for double flange-to-flange, dFF L2500 mm	138
Figure 5.16	Load deformation graph for dFF L2500	139
Figure 5.17	Ultimate capacity for double profile (dFF)	140
Figure 5.18	Calculation results for a double profile (dFF) based on EC-3	142
Figure 5.19	Two double profile flange-to-flange (2dFF)	147
Figure 5.20	Graphic section capacity of 2dFF	149
Figure 5.21	Four double profile flange-to-flange (4dFF)	150
Figure 5.22	Design capacity of 4dFF	151
Figure 5.23	Eight double profile flange-to-flange (8dFF)	152
Figure 5.24	Section capacity of 8dFF	153
Figure 5.25	Axial capacity of difference multiple sections	154
Figure 5.26	Compression test on 8dFF (l_e = 1000 mm)	156
Figure 5.27	Local buckling for 8dFF (l_e=1000 mm)	157
Figure 5.28	Experiment results for 8dFF (le=1000 mm)	157
Figure 5.29	Test layout for 8dFF le=1750 mm	158
Figure 5.30	End support for 8dFF L1750	159
Figure 5.31	Local bucking for 8dFF L1750-01	159
Figure 5.32	Local bucking for 8dFF L1750-02	160
Figure 5.33	Local bucking for 8dFF L1750-03	160
Figure 5.34	Experiment results for 8dFF L 1750 mm	161
Figure 5.35	Local buckling of 8dFF L 1750mm	161
Figure 5.36	Horizontal deflection for 8dFF L1750	162
Figure 5.37	Testing process for 8dFF L2500-01	163
Figure 5.38	Testing process for 8dFF L2500-02	164
Figure 5.39	Testing process for 8dFF L2500-03	165

Figure 5.40	Testing results of 8dFF L =2500 mm	166
Figure 5.41	Horizontal deflection of 8dFF L2500-01	166
Figure 5.42	Horizontal deflection of 8dFF L2500-02	167
Figure 5.43	Horizontal deflection of 8dFF L2500-03	167
Figure 5.44	Horizontal deflection of 8dFF L2500	168
Figure 5.45	Experimental results for 8dFF	168
Figure 5.46	Calculation results of combine profile 8dFF	170
Figure 5.47	Experiments vs calculations for 8dFF	172
Figure 5.48	Buckling curves (BS.EN1993-1-1, 2009)	178
Figure 5.49	Trend line for experimental results 8dFF	181
Figure 5.50	N experiment (N_{exp}) prediction based on the trend line experiment 8dFF	182
Figure 5.51	Reduction factor, ξ vs λ	183
Figure 5.52	Calculation part of α equation	184
Figure 5.53	Calculation result of α value	184
Figure 5.54	Adequate α value	185
Figure 5.55	Proposed buckling curve for 8dFF, $\alpha = 1.14$	188
Figure 5.56	Overlay buckling curve EC3 1-1 and experiment 8dFF	188
Figure 5.57	Plotting calculation with $\alpha = 1.14$	189

LIST OF ABBREVIATIONS

AISI	-	American Iron Steel Institute
AS/NZS	-	Autralian Standard/ New Zealand Standard
ASTM	-	American Society for Testing and Materials
BS	-	British Standard
BS EN	-	British adoption of a European (EN) standard
CFS	-	Cold-formed steel
dBB	-	Double/ combined profile back to back
dFF	-	Double/ combined profile flange to flange
dLL	-	Double/ combined profile lip to lip
DSM	-	Direct Strength Method
EC	-	Euro Code
EWM	-	Effective Width Method
HHWH	-	High Hex Washer Head
HWH	-	Hex washer head
LVDT	-	Linear Variable Differential Transformer
PPFH	-	Phillips Pan Framing Head
PPH	-	Philips pan head
TF	-	Tensile Flange section
TO	-	Tensile Original
TW	-	Tensile Web section

LIST OF SYMBOLS

A_0	-	Original cross-section area
a_0, a, b, c, d	-	Class indexes for buckling curves
A_{eff}	-	Effective area of a cross section
A_{net}	-	Net area of a cross section
b	-	Width of a cross section
C		Spring stiffness for rotation
d	-	Depth of straight portion of a web
E	-	Modulus of elasticity
e_0	-	Maximum amplitude of a member imperfection
F_{cr}	-	Elastic critical buckling load for global instability mode based on initial elastic stiffnesses
F_{Ed}	-	Design loading on the structure
f_u		Ultimate strength
f_y	-	Yield strength
f_{ya}	-	Average yield strength
f_{yb}	-	Basic yield strength
G	-	Shear modulus
h	-	Depth of a cross section
h	-	Storey height
h	-	Height of the structure
i	-	Radius of gyration about the relevant axis, determined using the properties of the gross cross-section
K	-	Spring stiffness for displacement
k	-	Factor for e0,d
L	-	Member length
l	-	Length
m	-	Number of columns in a row
M_{Ed}	-	Design bending moment
$M_{y,Ed}$	-	Design bending moment, y-y axis
$M_{y,Rd}$	-	Design values of the resistance to bending moments, y-y axis

$M_{z,Ed}$	-	Design bending moment, z-z axis
$M_{z,Rd}$	-	Design values of the resistance to bending moments, z-z axis
N_{cr}	-	Elastic critical force for the relevant buckling mode based on the gross cross sectional properties
N_{Ed}	-	Design value of the axial force
N_{Rd}	-	Design values of the resistance to normal forces
$N_{t,Rd}$	-	Design values of the resistance to tension forces
r	-	Radius of root fillet
t	-	Design core thickness of steel material before cold forming, exclusive of metal and organic coating
t_{cor}		The nominal thickness minus zinc and other metallic coating
t_f	-	Flange thickness
t_{nom}	-	Nominal sheet thickness after cold forming inclusive of zinc and other metallic coating not including organic coating
t_w	-	Web thickness
v	-	Poisson's ratio in elastic stage
x-x	-	Axis along a member
y-y	-	Axis of a cross-section
Z_{Ed}	-	Required design Z-value resulting from the magnitude of strains from restrained metal shrinkage under the weld beads
Z_{Rd}	-	Available design Z-value
z-z	-	Axis of a cross-section
α	-	Imperfection factor
α_h	-	Reduction factor for height h applicable to columns
α_m	-	Reduction factor for the number of columns in a row
γ_M	-	General partial factor
γ_{Mf}	-	Partial factor for fatigue
γ_{Mi}	-	Conversion factor particular partial factor
ε	-	Strain
ε_u	-	Ultimate strain
ε_y	-	Yield strain
λ	-	Non dimensional slenderness

λ_T	-	Relative slenderness for torsional or torsional-flexural buckling
λ_1	-	Slenderness value to determine the relative slenderness
σ	-	Stress
$\sigma_{com,Ed}$	-	Maximum design compressive stress in an element
Φ	-	Value to determine the reduction factor χ
χ	-	Reduction factor for the relevant buckling curve
$\varnothing$	-	Global initial sway imperfection
ρ	-	Reduction factor to determine reduced design values of the resistance to bending moments making allowance for the presence of shear forces
$\varnothing_0$	-	Basic value for global initial sway imperfection

LIST OF APPENDICES

APPENDIX	TITLE	PAGE
Appendix A	Tensile Test Results	203
Appendix B	Theoretical Calculations of Properties and Capacities of CFS	210
Appendix C	Design calculation of properties and capacities combine profile	237
Appendix D	Compression Test of Combined Profiles	245

CHAPTER 1

INTRODUCTION

1.1 Overview

A cold-formed steel (CFS) section is a type of steel section that has a thin profile, which means that the ratio of the width, b, or depth, h, over the thickness, t, of the profile is very large. Due to these relatively thin dimensions, the formation of the profile can be done using the cold forming process. In this process, the profile is formed from a steel plate or sheet into the desired shape at room temperature using a rolling machine or plate bending machine (press brake machine). The thickness of the plate that serves as the base material for forming the profile usually ranges between 0.4 mm (0.0149 in) and 6.4 mm (0.25 in) (Yu, 2010).

According to Yu (2011), the following qualities of CFS structural members distinguish them from other materials such as timber and concrete:

1. High strength, stiffness and lightness
2. Ease of fabrication and mass production
3. Fast and easy erection and installation; elimination of delays due to poor weather
4. Economic in transportation and handling
5. More accurate detailing and uniform quality
6. Low combustibility and recycled material.

The combination of the above-mentioned advantages can result in cost savings in construction.

Ye et al. (2016) also put forth the same argument that CFS wall systems, which have the advantage of being environmentally green and easy to construct, are commonly utilised as load-bearing structural components in low-rise and medium-rise structures and non-load bearing structural components in other residential, commercial and industrial buildings (Ye et al., 2016).

The utilization of CFS as wall-system for residential buildings is already very common, especially for single-story buildings (Figure 1.1). Its ease of implementation and proven structural strength have made CFS popular nowadays. However, limited land for constructing single-story buildings, which CFS is good for, might be the greatest obstacle in the effort to meet the housing needs. Due to this limitation, houses must be built using the conventional block system. So, the single-story building system becomes a multi-story building block system to accommodate growing housing needs.

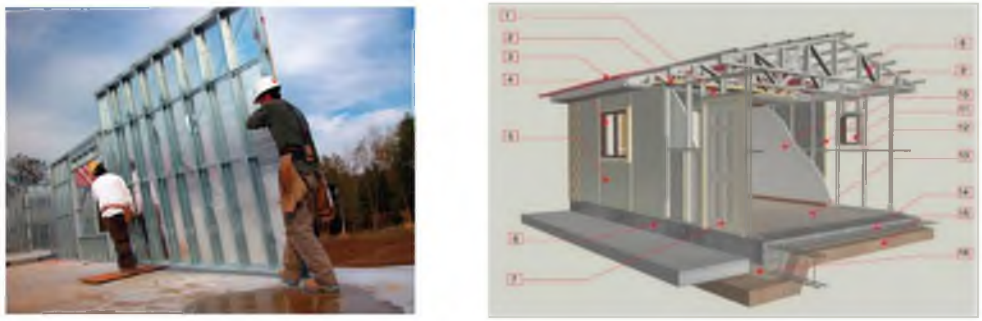

(a) (b)

Figure 1.1 (a). Wall-system installation (Alliance, 2007), (b). Single story building (Newfabksa, 2007)

For multi-story building system using CFS, a lot more needs to be done through the design manual that describes the structure of CFS. In the manual, it is stated that in a multi-story building, CFS is mostly intended to be used as a wall system and floor joist system. Meanwhile, for the main structural member, hot-rolled steel is still preferable (Lysaght, 2015; AS/NZS-4600, 2005; Australia Building Codes Board, 2006; Gardner, 2011).

It is also mentioned that the CFS does not function as the main structure but only as a wall-system only. Meanwhile, the main structure still uses a profile that serves as a hot-rolled steel framing (Figure 1.2).

The strength of a structure is influenced by the strength of the columns and the beams in its structural system. Columns have a more important function than beams in maintaining the strength of the structure. The destruction of a column will result in the destruction of the whole structure.

(a) (b)

Figure 1.2 (a) A CFS wall system (Alliance, 2007) and (b) a multi-story building structure used CFS as the wall system's main structure from steel profiles (www.greenmaltese.com).

The use of CFS in structures began to develop due to its light and easy in application and adequate strength (f_y = 550 N/mm^2), which is greater than that of normal hot-rolled steel (f_y = 275 N/mm^2). CFS is dominated by plastic behaviour, so it needs the strength limit if used as a structural column. These limits should be clearly defined through experimental studies so that CFS can be used as structural columns.

To get cold-formed sections that are suitable as structural columns, innovations of CFS materials need to be made through a wide variety of cold-formed profiles. CFS profiles will be fabricated and joined together so that the combined profile columns could at least withstand the structural loads of low-rise buildings, which experience relatively high loads compared to medium- or high-rise buildings.

A low-rise building in this study means a building that has four or fewer floors, as the use of a lift can be avoided in these cases, meaning that the desired effectiveness and efficiency of the building can be achieved. Such low-rise buildings are intended to be used as a residence or office buildings using a standard design load in accordance with the applicable regulations.

1.2 Background of the Study

The use of CFS sections as the main structural elements of a low-rise building is worth researching and developing. A column is an interesting subject because it is one element that is very important in low-rise buildings. Furthermore, one of the main requirements in multi-story buildings is to have strong columns (Dan Dubina, 2012; Yu, 1999).

The results of previous research (Figure 1.3) yielded information that CFS-based columns exhibit a variety of behaviours when subjected to axial load (Liu et al., 2017; Bernuzzi and Maxenti, 2015). There are differences in behaviour between single profile, double profile, and triple profile CFS-based columns (Madeira et al., 2015; Landesmann et al., 2016).

The shape of the single profile changes drastically after reaching the maximum axial load. The dominant behaviours on this type of profile are torsion and buckling (Figure 1.4). The experimental results have shown that the failure behaviour is torsion, followed by buckling, which leads to total collapse on both of the profiles. However, it is in contrast to the behaviour of the CFS double profile. This profile does not experience a significant torsional behaviour—however, buckling behaviour, which leads to a sudden total collapse, becomes the dominant behaviour of the CFS double profile.

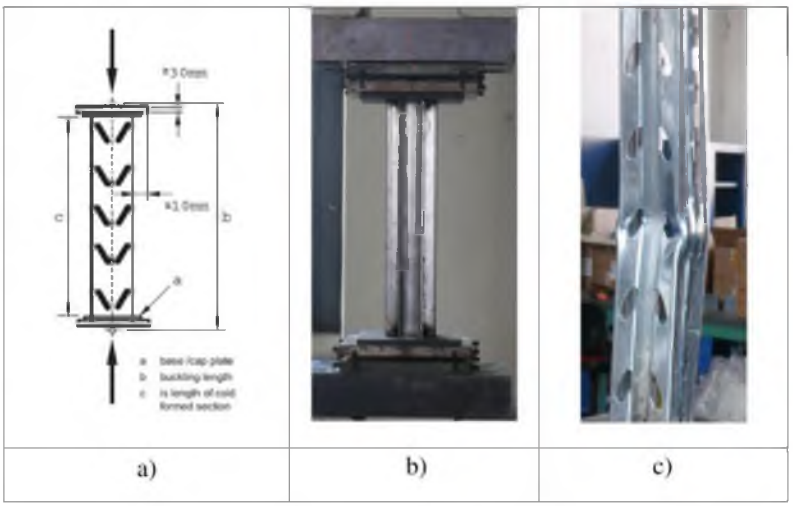

Figure 1.3 (a) Stub column test: details on the specimen, (b) the specimen before testing, and (c) typical failure due to local and distortional buckling (Bernuzzi and Maxenti, 2015).

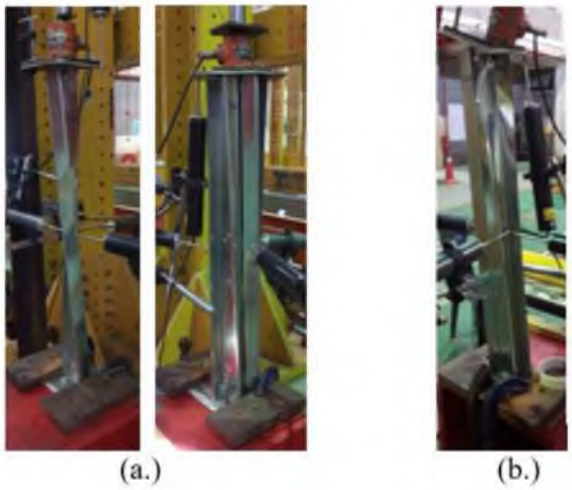

Figure 1.4 (a) Single and triple profile behaviour (torsional buckling dominated) and (b) double profile behaviour (local buckling dominated)

The results of the current study show that buckling behaviour is the main cause of the weakness of the section, especially in open section applications, leading to buckling and total collapses. Thus, the research related to the improved behaviour of CFS in the form of innovative combinations of CFS column profiles will be highly significant and beneficial. Innovation is required in order to reduce the buckling effect of the combined section. The proposed innovations of combined profiles to the CFS column section member is not only as compression member but also as the column structure. Besides, the distance and the strength of the plate stiffener should be detailed

in order to know the positive contribution of the plate stiffener installation profile on the CFS column.

The improved version of the CFS column will resist the low load level of the building structure, where the use of hot-rolled steel as columns can be avoided to improve the efficiency of low-rise buildings. Surely, this CFS column will provide convenience, not only in terms of implementation but also for mobilizing material from the manufacturer to the location of the fieldwork.

Additional research and analyses related to the use of CFS have been done. Experimental analyses and finite element approaches carried out by Ayhan (2015) and Schafer (2015) provide information that slenderness has a significant influence and needs to be considered in the usage of CFS in columns.

Some previous research suggests that there are some important things that still need to be investigated (C. C. Weng, 1990) regarding the contribution of stiffness to the rigidity of compression members. Ye Jihong (2016) found that CFS is still used only for single-level residential buildings and not multi-story building systems. However, Di Lorenzo *et al.* (2004) gave classification failures of CFS members that can be developed or combined to become strong members. Ayhan *et al.* (2015) commented that finite element analysis can be used to predict the design expression of CFS members. Therefore, this information could be used to extend such research to produce CFS columns that can carry greater loads, specifically for multi-story buildings.

1.3 Problem Statement

Combined profile columns have not been widely studied, especially those made of CFS. It is a significant problem to study because this kind of column is made from thin steel material and exhibits different behaviours than single profile columns.

The main problem associated with combined profile columns is that it is difficult to increase their resistance capacity and boost supporting parameters so that they can withstand the load from the floor above the column. Apart from buckling behaviour, column slenderness and spacing between self-drilling screws are important in determining the appropriate design of combined columns.

Analytical or theoretical methods may not provide sufficient and reliable information about the behaviours of combined profile columns. An experimental study is still needed to obtain accurate information based on the performance of combined profile columns.

Lastly, another question that arises is 'How can the capacity of a CFS section be increased from a combination of several similar profiles that are assembled into one unit with self-drilling screws as connectors in low-rise building structures?'

1.4 Objectives

The aim of this research is to investigate the behaviour of various types of columns formed by combining profiles CFS using self-drilling screws as connectors fixed along the columns. Subsequently, the objectives of this research can be listed as follows:

1. To determine the performance of the combined profile CFS column under compression.
2. To innovate various types of combined profiles of CFS using self-drilling screws as connectors between members.
3. To investigate the performance of columns made from a combined profile of CFS as a column with new parameters for low-rise buildings.

1.5 Scope of the Study

The present study will combine a model analysis based on a design code and an experimental model assessed in the laboratory. The scope of the study is divided into several stages:

1. Fundamental analysis and experimental testing of a single profile:

   To determine the behaviour of a single profile under compression using fundamental theory in CFS design, thus validating and comparing the model through experimental testing.

2. Analytical and experimental testing of combined profiles:

   To determine the behaviour of combined profiles, local buckling, flexural buckling, and torsional buckling.

3. Design and testing of screw connections for various spacing distances:

   To determine the suitable spacing between self-drilling screws as connectors for combined profile specimens. The arrangement and number of screws will be determined based on the code requirements.

4. Full-scale testing of combined profile CFS as a column:

   To determine the ultimate strength and failure modes of combined profile CFS as a column in the real conditions for a low-rise building structure.

1.6 Significances and Original Contributions of This Study

The results of this research are expected to illustrate some of the advantages and conveniences of using CFS in columns, including:

1. Combined columns provide an alternative to column structure of buildings that are conventionally constructed using hot-rolled steel or concrete columns.
2. Combined columns are expected to contribute as a load-bearing structure, especially in low-rise buildings.
3. Combined columns meet the guidelines of green buildings because they do not use excessive amounts of natural material. Also, waste material can be recycled to produce similar materials.

1.7 Organization of Thesis

This thesis is structured as follows: Chapter 2 contains the literature review, which covers basic theory and previous studies on CFS—specific topics include CFS used in columns, analyses and experiments involving CFS, the strength capacity of combined steel sections with screws. The last part of this chapter explains the gap identified in the literature. Chapter 3 discusses the analytical theory and stages of the experiment and the model test of the combined profile of CFS. Chapter 4 explains the mechanical properties of CFS, the experimental test of elasticity modulus, analytical experimental results, and chosen material properties that are used on the next stage. Then, the performance of combined profile CFS as a compression member is discussed—section properties are analysed and experiments are compared to determine the performance of combined profile CFS. The use of self-drilling screws as connectors for combined profile CFS is also discussed in this chapter. Chapter 5 presents the applied combined profile CFS as short columns for low-rise buildings, full-scale experiments, and analytical results to find the strength capacity of combined profile CFS with an adequate reduction factor. Finally, Chapter 6 provides conclusions and suggestions for future research.

REFERENCES

A G J WAY, M. D. H. 2012. *Design of Light Steel Sections to Eurocode 3*, The Steel Contruction Institute Silwood Park Ascot Berkshire, SL5 7QN.

AISI 2006. Cold-Formed Steel Frame and Beam-Column Design. *RESEARCH REPORTR P 0 3 - 2 American Iron and Steel Institute.*

ALLIANCE, S. F. 2007. SFA_Framing_Guide_final 2.

ANBARASU, M. 2016. Local-distortional buckling interaction on cold-formed steel lipped channel beams. *Thin-Walled Structures,* 98**,** 351-359.

AS/NZS-4600 2005. *ASNZS 4600-2005 ColdFormed Steel Structure,* Australia, Standards Australia Limited/Standards New Zealand.

ASTM-E8-01 2013. Standard Test Methods for Tension Testing of Metallic Materials. *Tention Testing of metallic material (sheet metal).* American Association State Highway and Transportation Officials Standard AASHTO No.: T68 An American National Standard.

ASTM 2013. Standard Test Methods for Tension Testing of Metallic Materials. ASTM.

AUSTRALIA BUILDING CODES BOARD, U. O. M., RONDO BUILDING SERVICES 2006. *Nash Standard Residential and Low-rise Steel Framing,* Victoria Australia.

BERNUZZI, C. & MAXENTI, F. 2015. European alternatives to design perforated thin-walled cold-formed beam–columns for steel storage systems. *Journal of Constructional Steel Research,* 110**,** 121-136.

BLUESCOPE 2014. section-properties-C75-C100.pdf. *In:* LYSAGHT, B. (ed.).

BONDOK, D. H. & SALIM, H. A. 2017. Failure capacities of cold-formed steel roof trusses end-connections. *Thin-Walled Structures,* 121**,** 57-66.

BRETTLE M E , D. G. B. 2009. *Steel Building Design: Concise Eurocode*, British Library Cataloguing-in-Publication Data.

BS.EN1993-1-1 2009. *BS EN 1993-1-1-2005+A1-2014 Eurocode 3 : Design of steel structure*

BS.EN1993-1-3 2006. *BS EN 1993-1-3-2006 Eurocode 3 Design of steel structure* British Stndard.

BSN 2013. *sni-7971-2013-struktur-baja-canai-dingin*.

C. C. WENG, T. P. 1990. Compression test of cfs steel column Journal of Structure ASCE. *Journal of Structure Engineering,* Vol. 116.

CAVA, D., CAMOTIM, D., DINIS, P. B. & MADEO, A. 2016. Numerical investigation and direct strength design of cold-formed steel lipped channel columns experiencing local–distortional–global interaction. *Thin-Walled Structures,* 105, 231-247.

CEN., E. C. F. S. 2011. EUROCODE en.1999.1.4.2007. *Eurocode 9: Design of aluminium structures - Part 1-4: Cold-formed structural sheeting,* EN 1999-1-4:2007/A1.

CHEN, M. & DENG, B. F. 2014. Analysis on Bearing Capacity of Axial Compression Short Column of Double Back-to-Back C Steel with Gusset Plates. *Applied Mechanics and Materials,* 501-504, 523-526.

CRAVEIRO, H. D., PAULO, J., RODRIGUES, C. & LAÍM, L. 2016a. Buckling resistance of axially loaded cold-formed steel columns. *Thin-Walled Structures,* 106, 358-375.

CRAVEIRO, H. D., RODRIGUES, J. P. C. & LAÍM, L. 2014. Cold-formed steel columns made with open cross-sections subjected to fire. *Thin-Walled Structures,* 85, 1-14.

CRAVEIRO, H. D., RODRIGUES, J. P. C. & LAÍM, L. 2016b. Experimental analysis of built-up closed cold-formed steel columns with restrained thermal elongation under fire conditions. *Thin-Walled Structures,* 107, 564-579.

DABAON, M., ELLOBODY, E. & RAMZY, K. 2015. Experimental investigation of built-up cold-formed steel section battened columns. *Thin-Walled Structures,* 92, 137-145.

DAN, D. 2014. Eurocodes_Steel_Workshop Cold-formed Steel Design. 65-70.

DAN DUBINA, V. U., RAFFAEL LANDOLFO 2012. *DESIGN OF COLD-FORMED STEEL STRUCTURES* Printed in Multicomp Lda, Mem Martins, Portugal, ECCS – European Convention for Constructional Steelwork, publications@steelconstruct.com, www.steelconstruct.com, WILEY BLACKWELL.

DI LORENZO, G. & LANDOLFO, R. 2004. Shear experimental response of new connecting systems for cold-formed structures. *Journal of Constructional Steel Research,* 60, 561-579.

DUBINA, D. 2014. Cold-formed Steel Design Eurocode 3 part 1-3

EL AGHOURY, M. A., SALEM, A. H., HANNA, M. T. & AMOUSH, E. A. 2015. Strength of cold formed battened columns subjected to eccentric axial compressive force. *Journal of Constructional Steel Research,* 113, 58-70.

GARDNER, L. 2011. *Stability of Steel beams and columns*, SCI, Silwood Park, Ascot, Berkshire. SL5 7QN UK.

GARIFULLIN MARSEL, N. U. 2015. Computational Analysis of Cold-formed Steel Columns with Initial Imperfections. *Procedia Engineering,* 117, 1073-1079.

GUNALAN, S., HEVA, Y. B. & MAHENDRAN, M. 2014. Flexural–torsional buckling behaviour and design of cold-formed steel compression members at elevated temperatures. *Engineering Structures,* 79, 149-168.

HAIDARALI, M. R. & NETHERCOT, D. A. 2012. Local and distortional buckling of cold-formed steel beams with edge-stiffened flanges. *Journal of Constructional Steel Research,* 73, 31-42.

HE, Z. & ZHOU, X. 2014. Strength design curves and an effective width formula for cold-formed steel columns with distortional buckling. *Thin-Walled Structures,* 79, 62-70.

HEURKENS, R. A. J., HOFMEYER, H., MAHENDRAN, M. & SNIJDER, H. H. 2018. Direct strength method for web crippling—Lipped channels under EOF and IOF loading. *Thin-Walled Structures,* 123, 126-141.

HILTI 2015. Product_Technical_Guide_for_Self_Drilling_Screws. *In:* HILTI (ed.) *Direct Fastening Technical Guide* www.us.hilti.com.

JOANNIDES, F. & WELLER, A. 2002. *Structural steel design to BS 5950*, Thomas Telford.

KEERTHAN, P. & MAHENDRAN, M. 2015. Improving the Shear Capacities of Lipped Channel Beams with Web Openings Using Plate Stiffeners. *Journal of Structural Engineering,* 141, 04015022.

LANDESMANN, A., CAMOTIM, D. & GARCIA, R. 2016. On the strength and DSM design of cold-formed steel web/flange-stiffened lipped channel columns buckling and failing in distortional modes. *Thin-Walled Structures,* 105, 248-265.

LI, Y.-L., LI, Y.-Q., SONG, Y.-Y. & SHEN, Z.-Y. 2016. In-plane behavior of cold-formed thin-walled beam-columns with lipped channel section. *Thin-Walled Structures,* 105, 1-15.

LIPING WANG AND BEN YOUNG, M. A. 2016. Behavior of Cold-Formed Steel Built-Up Sections with Intermediate Stiffeners under Bending. II: Parametric Study and Design. *Journal of Structural Engineering, © ASCE,*, J. Struct. Eng., 2016, 142(3): 04015151.

LIU, D., LIU, H., CHEN, Z. & LIAO, X. 2017. Structural behavior of extreme thick-walled cold-formed square steel columns. *Journal of Constructional Steel Research,* 128, 371-379.

LYSAGHT 2015. Lysaght Roofing Walling Installation Manual.

MADEIRA, J. F. A., DIAS, J. & SILVESTRE, N. 2015. Multiobjective optimization of cold-formed steel columns. *Thin-Walled Structures,* 96, 29-38.

MARTINS, A. D., CAMOTIM, D. & DINIS, P. B. 2017. Behaviour and DSM design of stiffened lipped channel columns undergoing local-distortional interaction. *Journal of Constructional Steel Research,* 128, 99-118.

MARTINS, A. D., DINIS, P. B. & CAMOTIM, D. 2016. On the influence of local-distortional interaction in the behaviour and design of cold-formed steel web-stiffened lipped channel columns. *Thin-Walled Structures,* 101, 181-204.

MOEN, C. D. & SCHAFER, B. W. 2008. Experiments on cold-formed steel columns with holes. *Thin-Walled Structures,* 46, 1164-1182.

MYCSI 2016. *MyCSI-SpecsForPCFS-Final_Rev5,* Miri, Sarawak Malaysia, Malaysia Cold-formed Steel Institute (MyCSI).

NEWFABKSA. 2007. The Saudi Company for Prefabricated Buildings LLC (NEWFAB).

NGUYEN, V. B., MYNORS, D. J., WANG, C. J., CASTELLUCCI, M. A. & ENGLISH, M. A. 2016. Analysis and design of cold-formed dimpled steel columns using Finite Element techniques. *Finite Elements in Analysis and Design,* 108, 22-31.

PEKOZ, T. 2012. COLD-FORMED_STEEL_STRUCTURES.

RACKFORD BONG, M. H. O. F. M. 2015. PERFORMANCE OF SINGLE LAP JOINTS USING ADHESIVE AND SELF-DRILLING SCREW FOR COLD-FORMED STEEL UNDER TENSILE LOADING. *Malaysian Journal of Civil Engineering.*

SCHAFER, B. W. 2008. Review: The Direct Strength Method of cold-formed steel member design. *Journal of Constructional Steel Research,* 64, 766-778.

SETIYAWAN, P. Cold-Formed Steel Technology in Building Structure and its Problems as an Alternative Solution of Corrosion Resistant Structures at Coastal Areas. International Conference on Coastal and Delta Areas, 2015. 263-272.

SREEDHAR KALAVAGUNTA, S. N., KAMAL NASHARUDDIN BIN MUSTAPHA 2013. Experimental Study of Axially Compressed Cold Formed Steel Channel Column. *Indian Journal od Science and technology,* 06 (04)

SREEDHAR KALAVAGUNTA, S. N. A. K. N. B. M. 2012. Pushover Analysis for Cold Formed Storage Rack Structures jordan journal of civil engineering. *Jordan Journal of Civil Engineering,* Volume 6, 490-500.

UMM, J. S. 2016. Proposal KJI XII Form Identitas KJI 2016.pdf>.

VIJAYANAND, S. & ANBARASU, M. 2017. Effect of Spacers on Ultimate Strength and Behavior of Cold-Formed Steel Built-up Columns. *Procedia Engineering,* 173, 1423-1430.

WAN, H.-X. & MAHENDRAN, M. 2015. Behaviour and strength of hollow flange channel sections under torsion and bending. *Thin-Walled Structures,* 94, 612-623.

WANNIARACHCHI, K. S. & MAHENDRAN, M. 2017. Experimental study of the section moment capacity of cold-formed and screw-fastened rectangular hollow flange beams. *Thin-Walled Structures,* 119, 499-509.

WEI-WEN YU, R. A. L. 2011. *COLD FORMED STEEL DESIGN FOURTH EDITION.*

YE, J., FENG, R., CHEN, W. & LIU, W. 2016. Behavior of cold-formed steel wall stud with sheathing subjected to compression. *Journal of Constructional Steel Research,* 116, 79-91.

YE, J., HAJIRASOULIHA, I. & BECQUE, J. 2018. Experimental investigation of local-flexural interactive buckling of cold-formed steel channel columns. *Thin-Walled Structures,* 125, 245-258.

YOUNG, B. 2008. Research on cold-formed steel columns. *Thin-Walled Structures,* 46, 731-740.

YU, W.-W. 1999. Cold-formed steel structures *In:* WAI-FAH, C. (ed.) *Structure Engineering Handbook.* Boca Raton: CRC Press LLC, 1999.

YU, W. W. 2010. Cold-Formed Steel Structure Design. *John Wiley and Sons, Inc,* 17-32.

ZEYNALIAN, M., SHELLEY, A. & RONAGH, H. R. 2016. An experimental study into the capacity of cold-formed steel truss connections. *Journal of Constructional Steel Research,* 127, 176-186.

ZHANG, J.-H. & YOUNG, B. 2015. Numerical investigation and design of cold-formed steel built-up open section columns with longitudinal stiffeners. *Thin-Walled Structures,* 89, 178-191.

ZHENG, B., HUA, X. & SHU, G. 2015. Tests of cold-formed and welded stainless steel beam-columns. *Journal of Constructional Steel Research,* 111, 1-10.

ZHU, A., ZHU, H., ZHANG, X. & LU, Y. 2016. Experimental study and analysis of inner-stiffened cold-formed SHS steel stub columns. *Thin-Walled Structures,* 107, 28-38.

LIST OF PUBLICATIONS

1. Septiropa, Z., Osman, M. H., and Abd. Rahman, A. B. (2018). *Basic performance combines profile of cold-formed steel as the basis for design compression member*. International Conference on Durability of Building and Infrastructures, 10-12 January 2018, Sarawak, Malaysia.
2. Septiropa, Z., Osman, M. H., Abd. Rahman, A. B., Mohd Ariffin, M. A., Huda, M., and Maselono, A. (2018). Profile of cold-formed steel for compression member design a basic combination performance. *International Journal of Engineering and Technology*, *7*(2.27), 284-290. https://doi.org/10.14419/ijet.v7i2.27.15807
3. Septiropa, Z., Osman, M. H., Abd. Rahman, A. B., and Mohd Ariffin, M. A. (2019). Effect of screw distance on combined profiles cold-formed steel in increasing the compression member capacity. *IOP Conference Series: Materials Science and Engineering*, *527*, 012080. https://doi.org/10.1088/1757-899X/527/1/012080